1

A LEVEL SET APPROACH FOR DILUTE FLUID-PARTICLE FLOWS

HAILIANG LIU AND ZHONGMING WANG

Abstract. Gas-particle and other dispersed-phase flows can be described by a kinetic equation containing terms for spatial transport, acceleration, and particle processes (such as evaporation or collisions). However, computing the dispersed velocity is a challenging task due to the large number of independent variables. A level set approach for computing dilute fluid-particle flows is presented. We will consider the sprays governed by the Williams kinetic equation with the initial distribution of the form $\sum_{i=1}^{N} \rho_i(x)\delta(\xi - u_i(x))$. The dispersed velocity is described as the zero level set of a smooth function, which satisfies a transport equation. This together with the density weight recovers the particle distribution at any time. Moments of any desired order can be evaluated by a quadrature formula involving the level set function and the density weight. It is shown that the method can successfully handle highly non-equilibrium flows (e.g. impinging particle jets, jet crossing, particle rebound off walls, finite Stokes number flows).

Contents

1. Introduction

The numerical simulation of two-phase flows composed of a cloud of particles in a gas/fluid flow was the object of many studies in the past years, e.g., the dispersion of dusts and smokes [14], biomedical flows [3, 5] and combustion [1, 2, 19, 25, 33]. In order to model these kind of flows, one can essentially use two approaches: a kinetic one or a fluid one. In the kinetic model, the spray is described by a distribution function $f(t, x, \xi)$ which takes into account of the position x of a particle, and its velocity ξ. When function $f(t, x, \xi)$ is a Gaussian function in terms of ξ, the kinetic model can be reduced to a fluid one. But for non-equilibrium flows, the solution

[1]Discussion with Rodney Fox

Date: November 11, 2009.

method must be derived from the kinetic description since the fluid model can not handle locally multiple velocities observed in the particle trajectory crossing process.

We are interested in construction of numerical methods for non-equilibrium flows wherein the velocity density function is far from Maxwellian. For example, dilute systems often exhibit non-equilibrium behavior because particle collisions are too weak to overcome kinetic effects. In many cases the velocity density function can be non-unimodal, implying that there is a high probability of finding particles with distinctly different velocities at the same location. Such behavior can be easily captured in the Lagrangian simulation and is known as particle-trajectory crossing (PTC).

In this paper a level set method is developed for capturing the PTC phenomena in poly-disperse multiphase flows. As an example we will consider sprays in a compressible gas flow. The sprays are governed by a kinetic equation for particle distribution functions. Instead of solving the full kinetic equation or classical moment equations [11, 22], we intend to implicitly capture velocity field of dispersed particles in phase space using a level set approach. All particle velocities will be identified as the zero level sets of smooth functions.

As pointed out in [10], standard moment methods have great difficulty treating systems with aggregation and breakage. The Lagrangian particle tracking method has been widely used for sprays [13]. The treatment of dispersed phase with finite Stokes number introduces the additional complication of accounting for the dispersed-phase velocity. In the Lagrangian formulation, this is done by solving for the particle velocity as it transverses the (Eulerian) gas phase. Although accurate, this solution method is rather expensive and subject to statistical errors due to finite sample sizes. Similar to the quadrature method of moments (QMOM) developed in [29], recently the direct quadrature method of moments (DQMOM) [15, 16, 17, 28] has been developed as an Eulerian method, which solves an Eulerian model where each quadrature node has its own velocity field. The number of moments needed to form a closed system of transport equations is $N(d+1)$ with N particle velocities in d spatial dimension. The comparison between the Lagrangian particle tracking method and the DQMOM method in [18] showed excellent agreement between quantities such as the droplet number density and mass density. The computational cost of the DQMOM is lower than the Lagrangian method, and this leads to an ongoing active development. However, complications occur when one needs to add more particle clusters (larger N) to the initial set up. These problems are amplified when solving a high dimensional problem.

The main topic investigated in this work is the treatment of velocity dispersion by using the level set methodology. As an example, we consider a laminar spray. The mathematical model is given by the Williams equation [33] for the velocity ξ, number density function $f(t, x, \xi)$ as

$$\partial_t f + \xi \cdot \nabla_x f + \nabla_\xi \cdot (fF/m_p) = Q, \tag{1.1}$$

where F is the drag force acting on a droplet, m_p is the droplet mass, and Q is the collisions/coalescence term. Note that extending f to include other variables (e.g., droplet temperature, chemical composition, etc) is straightforward if the appropriate rate expressions are added to (1.1). In the very simple case of mono-disperse particulate phase (with no collisions, secondary atomization, not turbulent dispersion), this equation reads

$$\partial_t f + \xi \cdot \nabla_x f + \nabla_\xi \cdot (fF/m_p) = 0,$$

which will be used to formulate our level set method. The kinetic equation is often coupled with the following compressible system

$$\partial_t \rho + \nabla_x \cdot (\rho u) = 0,$$
$$\partial_t(\rho u) + \nabla_x \cdot (\rho u \otimes u + P(\rho)I) = -\int F f d\xi,$$

where for perfect gases

$$P(\rho) = A\rho^\gamma, \quad A > 0 \quad \text{and} \quad \gamma > 1.$$

The existence and uniqueness as well as the stability of this model are studied in [4, 12, 21].

In general, PTC does not occur at zero Stokes number, but can occur beyond a critical Stokes number when the particles are no longer able to follow the fluid. For small Stokes number, one usually explore the Eulerian model for gas-particle flows by taking the leading moments with closure assumption $f = n\delta(\xi - v(t,x))$:

$$n(t,x) = \int_{R_\xi} f(t,x,\xi)d\xi, \quad nv = \int_{R_\xi} \xi f(t,x,\xi)d\xi,$$

which leads to a pressure-less system

$$\partial_t n + \nabla_x \cdot (nv) = 0,$$
$$\partial_t (nv) + \nabla_x \cdot (nv \otimes v) = ng + \frac{n}{m_p} F(u,v).$$

In the context of turbulence, the pressure-less model fails to reproduce the spreading of particles, even it is coupled with a turbulence model for the fluid. The partial remedy for this problem is to take a Gaussian-shape closure assumption (see [31] for related work)

$$f(t,x,\xi) = \frac{n(x,t)}{(2\pi\sigma(x,t))^{d/2}} \exp\left(\frac{|\xi - v(x,t)|^2}{2\sigma^2}\right),$$

where σ is particle-velocity standard deviation, and by introducing additional diffusion terms in the governing kinetic equation. The simplest such model is

$$\partial_t f + \nabla_x \cdot (\xi f) + \nabla_\xi \cdot (fF/m_p) - \nabla_\xi \cdot (D\nabla_\xi f) = 0,$$

where D is a positive coefficient depending upon the properties of the fluid turbulence. We refer to [6, 7, 9, 20] and references therein for modeling and computational aspects in this regime.

We note that taking the moments and using the closure assumption, one obtains a hyperbolic system, which does not display the measure-valued concentration observed in the pressure-less system. Also because of the closure assumption the system is not adapted to reproduce strongly non-equilibrium situations such as jet crossing, jet-wall interaction etc, and leads in those cases to non-physical solutions.

The level set approach developed here handles more general closure assumptions. This approach allows for large number of particle clouds in arbitrary dimension. The important feature of our method is that we use only one level set function to capture all possible velocities, and any higher moments can be easily evaluated in a post-processing step if desired.

2. Description of Algorithm

2.1. **Kinetic transport equations.** In our study we shall consider the kinetic equation for a non-evaporating, mono-disperse particulate phase (with no collisions, secondary atomization, not turbulent dispersion). We shall denote the particle number density function by $f(t,x,\xi)$ in the phase space $(x,\xi) \in \mathbb{R}^d \times \mathbb{R}^d$, and the force acting on a particle by F. The equations of transport are given by the Williams' equation [33]

$$\partial_t f + \xi \cdot \nabla_x f + \nabla_\xi \cdot (fF/m_p) = 0, \tag{2.1}$$

where m_p denotes the mass of a particle. This model governs the particle evolution at the kinetic level in a d-dimensional physical space with particle velocity ξ and position x. All the relevant physics can in theory be included in this equation or its variant.

If one assumes that the particle density is much greater than the fluid density (e.g., solid or liquid particles suspended in a gas), the expression for F is quite simple, and corresponds (in an initial force) to the sum of the drag force and the gravity force (often ignorable). Hence one has

$$F(u,\xi) = \frac{1}{2}\pi r^2 \rho C_d |u(t,x) - \xi|(u(t,x) - \xi) + m_p g,$$

where u is the fluid velocity, r is the particle radius, ρ the fluid density, and C_d the particle drag coefficient given by the following correlation due to Schiller and Naumann [32]:

$$C_d = \frac{24}{Re}(1 + Re^{2/3}),$$

with $Re = 2\rho|u - \xi|r/\mu$ being the particle Reynolds number where μ is the dynamic viscosity of the fluid. Thus the basic form of the force F is given by

$$F = C(u(t, x) - \xi).$$

A conventional way to solve the kinetic equation is to use moment method to solve a system of moments. The moment system is often not closed, and an assumption on the shape of the number density function has to be made to form a closed system. For very small Stokes numbers, a simple assumption is

$$f = n\delta(\xi - v(x, t)).$$

One hence explores the Eulerian model for gas-particle flows by taking the leading moments with this closure assumption

$$n(x, t) = \int_{R_\xi} f(t, x, \xi)d\xi, \quad nv = \int_{R_\xi} \xi f(t, x, \xi)d\xi,$$

which leads to a pressure-less system

$$\partial_t n + \nabla_x \cdot (nv) = 0,$$
$$\partial_t(nv) + \nabla_x \cdot (nv \otimes v) = ng + \frac{n}{m_p}F(u, v).$$

However, this model suffers a major drawback, by the closure assumption, it is unable to take into account the presence of particles with different velocities located at the same point. This can lead to nonphysical results in the case of two crossing jets of particles, or in the case of a jet of particles impinging on a wall. This is not surprising since this model is not well-posed in the usual function spaces L^∞ or L^1 even in one-dimensional case, and cannot capture the particle-trajectory crossing (PTC) phenomena.

2.2. **Level set description.** Since $v(t, x)$ is expected to become multi-valued when particle trajectory crosses, conventional moment closure will incur inaccurate prediction when solving the kinetic equation. Instead, we shall use the level set technique to flexibly capture the particle-trajectory crossing. The usual closure method is derived by considering the concentrated data

$$f(t, x, \xi) = n(x, t)\delta(\xi - v(t, x)).$$

Such a concentration will propagate in phase space, with information concentrated only on a manifold. This observation leads to an effective level set description. The methodology follows from level set techniques developed for computing physical observables in high frequency wave propagation problems, see e.g. [24, 23, 26, 27].

Our level set function is denoted as $\phi = \phi(t, x, \xi)$. Therefore all velocities are collectively represented as zero level set of ϕ, i.e.,

$$\phi(t, x, v(t, x)) \equiv 0.$$

This representation remains valid even $v(t, x)$ becomes multi-valued, while

$$v(x, t) \in \{\xi, \quad \phi(t, x, \xi) = 0\}.$$

With this level set function we seek the solution of the following form

$$f(t, x, \xi) = \rho(t, x, \xi)\delta(\phi(t, x, \xi)),$$

where ρ serves to capture the weights of density distributions. Substitution of this ansatz into the William equation (2.1) leads to

$$\delta(\phi)a + \delta'(\phi)\rho b = 0, \tag{2.2}$$

where

$$\partial_t \rho + \xi \cdot \nabla_x \rho + \nabla_\xi \cdot (\rho F/m_p) = a,$$
$$\partial_t \phi + \xi \cdot \nabla_x \phi + F/m_p \cdot \nabla_\xi \phi = b.$$

In order to ensure (2.2) to hold for any (t, x, ξ) it suffices to take $a \equiv 0$ and $b \equiv 0$ for $\rho \not\equiv 0$. This leads to the key level set equation

$$\partial_t \phi + \xi \cdot \nabla_x \phi + F/m_p \cdot \nabla_\xi \phi = 0, \tag{2.3}$$

which can be computed near the neighborhood of $\phi = 0$, as well as a transport equation for the weight ρ:

$$\partial_t \rho + \xi \cdot \nabla_x \rho + \nabla_\xi \cdot (\rho F/m_p) = 0. \tag{2.4}$$

We thus can state the following.

Theorem 2.1. *Let ϕ be the solution to (2.3) subject to initial data $\phi(0, x, \xi)$, and ρ be the solution to (2.4) with initial data $\rho(0, x, \xi)$, then*

$$f(t, x, \xi) = \rho(t, x, \xi)\delta(\phi(t, x, \xi))$$

is the solution of the William equation (2.1) with initial distribution of the form $\rho(0, x, \xi)\delta(\phi(0, x, \xi))$.

2.3. **Initialization.** Special care must be taken when constructing initial data for the above level set equation and the density transport equation. Let the set of particle clouds be denoted by J_i with $\cup_{i=1}^N J_i \subset \Omega$, corresponding particle density $\rho_i(x)$ and velocity $u_i(x)$. The initial distribution of particles can be expressed as an expansion of the number density function in a sum of weighted delta functions in phase spaces [16]:

$$f(0, x, \xi) = \sum_{i=1}^N \rho_i(x)\chi(J_i)\delta(\xi - u_i(x)).$$

From this expression it follows that for $x \in J_k$

$$\rho_k(x) = \int f(0, x, \xi)d\xi, \quad u_k(x) = \frac{\int \xi f(0, x, \xi)d\xi}{\int f(0, x, \xi)d\xi}.$$

Thus we say the above choice of the initial distribution is admissible.

We now turn to construction of a level set function $\phi(0, x, \xi)$ so that

$$\bigcup_{i=1}^N \{(J_i, \xi), \quad \xi = u_i(x)\} = \{(x, \xi), \quad \phi(0, x, \xi) = 0\}.$$

Note that in contrast to the classical level set formulation [30], here the zero level set is not necessarily a closed curve or surface, but a set of collected points or regions.

Note that the initial choice of $\phi(0, x, \xi)$ is not unique. Unless otherwise specified, we shall use the distance function to initialize the velocity field as follows:

$$\phi_0(x, \xi) := \phi(0, x, \xi) = \min_i \min_{y \in J_i} \sqrt{|x - y|^2 + |\xi - u_i(y)|^2}. \tag{2.5}$$

The cost for a direct computation is about $O(NM^{2d}M_J^d)$, where M is the number of grid points in each direction, and M_J denotes the number of grid points in the set where particle clouds are located. The complexity is small if there is only small number of particles.

Next we construct a density weight function $\rho(0, x, \xi) > 0$ so that

$$\rho(0, x, \xi)\delta(\phi(0, x, \xi)) = \sum_{i=1}^N \rho_i(x)\chi(J_i)\delta(\xi - u_i(x))$$

in distributional sense. We take

$$\rho_0(x,\xi) := \rho(0,x,\xi) = \sum_{i=1}^{N} \rho_i(x)|\partial_\xi \phi_0|_{\xi=u_i(x)}\chi(J_i)$$

so that for any smooth test function $V \in C_0^\infty(\mathbb{R}^d)$ we have

$$\int \rho_0(x,\xi)\delta(\phi_0(x,\xi))V(\xi)d\xi = \sum_{i=1}^{N} \rho_i(x)\chi(J_i).$$

2.4. **Post-processing.** Once having solved the above equations we are in a position to evaluate the desired physical quantities. The zero level set of $\phi(t,x,\xi)$ gives multiple velocities at location x and time t:

$$v(t,x) \in \{\xi, \quad \phi(t,x,\xi) = 0\}.$$

Note that as time evolves ϕ can become flat and small simultaneously, this would bring difficulties to identify a sharp set of zeros of ϕ. In this case, higher order interpolation may be used to determined the zero level set.

The velocity moments of any order can be obtained in the following post-precessing step, for example,

$$M^0(t,x) = \bar{n}(x,t) = \int_{R_\xi} \rho\delta(\phi)d\xi, \quad M_i^1(t,x) = \int_{R_\xi} \xi_i \rho\delta(\phi)d\xi.$$

It can be shown as in [27] that for N velocities v_α with density n_α, we have

$$\bar{n}(x,t) = \sum_{\alpha=1}^{N} n_\alpha, \quad \bar{v} = \frac{\sum_{\alpha=1}^{N} n_\alpha v_\alpha}{\sum_{\alpha=1}^{N} n_\alpha}.$$

Note that using moment closure method one needs at least $N(d+1)$ moments to resolve the desired number of velocities and associated densities. The main advantage of the level set method described above is its ability to capture all emerging velocities and densities in an implicit manner. Moments of any desired order can be evaluated in a post-processing step. It is demonstrated in the numerical examples.

2.5. **Summary.** We can now summarize our algorithm.

Step 1. Initialize ϕ_0 to be a distance function to the initial velocity distribution of particles, as well as the density weight $\rho_0(x,\xi)$

Step 2. Solve the level set equation

$$\partial_t \phi + \xi \cdot \nabla_x \phi + F/m_p \cdot \nabla_\xi \phi = 0,$$

for one time step. The computation is done in the neighborhood of $\phi = 0$. Denote the update ϕ by ϕ^{n+1}.

Step 3. Solve the transport equation

$$\partial_t \rho + \nabla_x \cdot (\xi\ \rho) + \nabla_\xi \cdot (\rho F/m_p) = 0,$$

to obtain ρ^{n+1}.

Step 4. We have now advanced one time step. The zero level set of ϕ^{n+1} gives the new multiple velocity, and the density weight ρ^{n+1}. Repeat steps 2 and 3.

Step 5. At the final time, multiple velocities are determined by the contour plot $\phi = 0$ for any (t,x).

Step 6. Evaluation of physical quantities: total tensity and mean velocity of particles.

$$\bar{n}(x,t) = \int_{R_\xi} \rho\delta(\phi)d\xi, \quad \bar{v} = \int_{R_\xi} \xi\rho\delta(\phi)d\xi/\bar{n}(x,t),$$

where the Dirac$-\delta$ function is approximation by δ_ϵ

$$\delta_\epsilon^{\cos}(x) = \frac{1}{2\epsilon}\left(1 + cos\left(\frac{\pi x}{\epsilon}\right)\right) I_{[-\epsilon,\epsilon]}, \tag{2.6}$$

with ϵ to measure the support of the δ function. ϵ is usually proportional to the spatial mesh size $\Delta\xi$. In our simulation, ϵ is taken to be $\Delta\xi$ or $2\Delta\xi$.

3. Discretization

Because of the transport form of the system for the level set function, and the conservative form for the density weight, we shall use finite difference and finite volume method for these two systems respectively. For the sake of clarity, let us begin by considering the one-dimensional in x case, the multi-dimensional extension being straightforward.

A uniform mesh will be used for the density weight and the level set function. With Δx and $\Delta\xi$ as the mesh size in x and ξ direction, we define

$$\begin{aligned}
&x_i = i\Delta x, \xi_j = j\Delta\xi.\\
&\rho_{i,j} = \rho(x_i, \xi_j),\\
&\phi_{i,j} = \phi(x_i, \xi_j),\\
&i = 0, \cdots M-1,\\
&j = 0, \cdots N-1.
\end{aligned}$$

3.1. **Second order finite difference (FD) scheme for the level set equation.** We use a second order Range-Kutta method for evolving the level set equation in time, and high-resolution upwind method for spatial transport. In order to present the numerical scheme in explicit manner, here and in what follows we use following notations: $D_x^\pm$ denote finite difference operators in $x-$direction.

$$D_x^+\phi_j = \frac{\phi_{j+1} - \phi_j}{\Delta x} = D_x^-\phi_{j+1}, \quad D_x^0\phi_j = \frac{\phi_{j+1} - \phi_{j-1}}{2\Delta x}.$$

The difference operator in ξ direction is similarly defined. Here and in what follows we shall use the following notation

$$g^+ = \frac{1}{2}(|g| + g), \quad g^- = \frac{1}{2}(g - |g|)$$

to denote both positive and negative part of the quantity, respectively.

The solution is firstly advanced to the full time step using the forward Euler method as a prediction

$$\phi_{j,k}^* = \phi_{j,k}^n - \Delta t L[\phi]_{j,k}^n, \tag{3.1}$$

where

$$L[\phi] := \left[\xi_k^+\tilde{D}_x^-\phi + \xi_k^-\tilde{D}_x^+\phi + F^+\tilde{D}_\xi^-\phi + F^-\tilde{D}_\xi^+\right].$$

Here Δt is the time step, j and k denote the grid indices and n dentoes the time interval. The difference operator $\tilde{D}$ is restricted by limiters to preserve certain monotonicity. In our computation we use a second order ENO limiter.

Define

$$m(a, b) = \begin{cases} a & \text{if } |a| \le |b|, \\ b & \text{otherwise.} \end{cases}$$

We now have for $h = \Delta x$

$$\begin{aligned}
\tilde{D}_x^-\phi_j &= D_x^-\phi_j + hm(D_x^+D_x^-\phi_{j-1}, D_x^+D_x^-\phi_j)/2,\\
\tilde{D}_x^+\phi_j &= D_x^+\phi_j - hm(D_x^+D_x^-\phi_j, D_x^+D_x^-\phi_{j+1})/2.
\end{aligned}$$

The numerical solution at next time step is determined by

$$\phi_{j,k}^{n+1} = \frac{1}{2}\phi_{j,k}^n + \frac{1}{2}\phi_{j,k}^* - \frac{\Delta t}{2}L[\phi^*]. \tag{3.2}$$

3.2. **Second-order finite volume (FV) scheme for density transport.** Let $I_{j,k} = I_j \times I_k$ be a control volume with $I_j = [x_{j-1/2}, x_{j+1/2}]$ and $I_k = [\xi_{k-1/2}, \xi_{k+1/2}]$; and $\rho_{j,k}$ be the cell average over $I_{j,k}$. In each $I_{j,k}$, the solution representative is a first order polynomial

$$p[\rho]|_{I_{j,k}} = \rho_{j,k} + s'_{j,k}(x - x_j) + s^{\backprime}_{j,k}(\xi - \xi_k),$$

with slopes chosen as

$$s'_{j,k} = mm(D_x^+\rho_{j,k}, D_x^-\rho_{j,k}), \quad s^{\backprime}_{j,k} = mm(D_y^+\rho_{j,k}, D_y^-\rho_{j,k}).$$

Thus the semi-discrete scheme can be written as

$$\frac{d}{dt}\rho_{j,k} + \frac{\widehat{(\xi\rho)}_{j+1/2,k} - \widehat{(\xi\rho)}_{j-1/2,k}}{\Delta x} + \frac{\widehat{(F\rho)}_{j,k+1/2} - \widehat{(F\rho)}_{j,k-1/2}}{\Delta \xi} = 0. \tag{3.3}$$

Classical upwind numerical fluxes are adopted as

$$\widehat{(\xi\rho)}_{j+1/2,k} = \xi_k^+(\rho_{j,k} + \frac{\Delta x}{2}s'_{j,k}) + \xi_k^-(\rho_{j+1,k} - \frac{\Delta x}{2}s'_{j+1,k}), \tag{3.4}$$

$$\widehat{(F\rho)}_{j,k+1/2} = F^+(t, x_j, \xi_{k+1/2})(\rho_{j,k} + \frac{\Delta y}{2}s^{\backprime}_{j,k}) + F^-(t, x_j, \xi_{k+1/2})(\rho_{j,k+1} - \frac{\Delta y}{2}s^{\backprime}_{j,k+1}). \tag{3.5}$$

Now the semi-discrete scheme is a closed ODE system for cell averages $\{\rho_{j,k}\}$. A second order Runge-Kutta method is applied for time discretization.

3.3. **Multi-dimensional extension.** The multidimensional extension of the scheme we just described follows naturally using dimension-by-dimension handling. Indeed, the level set equation and density transport equation have already been derived for multiple dimensions, and the computation of numerical fluxes in multi-dimensional case is essentially the same as described above. Details are omitted.

4. Numerical Results for example applications

In this section we apply our level set algorithm to non-equilibrium fluid-particle flows in order to illustrate its ability to handle non-trivial problems. We will consider the case without drag force (or equivalently infinite Stokes) and the case with given drag forces for a range of Stokes numbers. The complex case with drag-force computed from a coupled gas dynamic system will be considered elsewhere.

4.1. **One-dimensional test cases.** *1. Impinging particles*
The first flow that we consider is one-dimensional with two particle "packets" moving in opposite directions. The particles are collisionless and not affected by any drag forces.

For these two particles, we give initial density and velocity as follows:

$$\rho_0(x) = \frac{1}{3}\delta(x - 0.25) + \frac{2}{3}\delta(x - 0.75), \quad u_0(0.25) = 1, \quad u_0(0.75) = -1.$$

In the simulation the computation domain is chosen as $[0, 1] \times [-1.1, 1.1]$. In the initialization step we take $f(0, x, \xi) = \rho_0(x, \xi)\delta(\phi_0(x, \xi))$, where

$$\phi_0(x, \xi) = \xi - u_0^\epsilon(x),$$

$$\rho_0(x, \xi) = \rho_0^\epsilon(x),$$

where $(\rho_0^\epsilon, u_0^\epsilon)$ are the approximation of (ρ_0, u_0) using cosine kernel, i.e.,

$$\rho_0^\epsilon = \frac{1}{3}\delta^\epsilon(x - 0.25) + \frac{2}{3}\delta^\epsilon(x - 0.75), \delta^\epsilon(y) = \frac{1}{2\epsilon}(1 + cos(\pi y/\epsilon))I_{[-\epsilon,\epsilon]}(y)$$

and

$$u_0^\epsilon(x) = \begin{cases} 1 & |x - 0.25| \le \epsilon, \\ -1 & |x - 0.75| \le \epsilon, \end{cases}$$

where ϵ is the same as that used to approximate the two Dirac delta function. A constant extension is used to impose the boundary condition. The two packets will thus eventually collides at $t = 0.25$. The results are shown in Fig.1 at time 0.1, 0.2, 0.3 and 0.4. We see that two particles before and after collision at time 0.2 and 0.3, respectively. The example shows the capability of our numerical method in capturing the PTC phenomenon.

2. Three clouds of particles

This example illustrates the crossing behavior of three clouds of particles. The initial setting is as follows:

$$u_0(x) = \begin{cases} 0.5 & x \le 0.2, \\ 0 & 0.4 \le x \le 0.6 \\ -0.5 & x \ge 0.8, \end{cases}$$

$$\rho_0(x) = 0.5\chi_{x\le 0.2} + 1.0\chi_{0.4\le x\le 0.6} + 1.5\chi_{x\ge 0.8}$$

The computation domain is $[0,1]\times[-0.75, 0.75]$. The distance function is used to initialize ϕ. A constant boundary condition is used to mimic the particle flow gets in/out. It's easy to know from the initial conditions that At time $t = 0.4$, particles will collide at $x = 0.6$ and $x = 0.8$. We present the density at $t = 0.1, 0.5, 0.7, 1.0$ in Fig. 2 before and after the collision. Before collision, at $t = 0.1$, we see the movement of the particle clouds. After the first collision at $x = 0.6$ and $x = 0.8$, we observed the superposition of the density of two clouds at time $t = 0.5$. After the second collision at $x = 0.5$, we see the superposition of the density of three clouds at $t = 0.7, 1.0$. These observations are confirmed by the velocity plots as well in in Fig. 2.

This examples shows that, unlike the moment closure method and DQMOM method, which need more equations or nodes when more particle velocities are presented, the level set method handles multi-velocity automatically.

3. Finite stokes number

The previous two examples simulate the free motion (infinite Stokes number) of clouds of particles without coupling fluid. They demonstrate the capability and simplicity of our level set method in describing the non-equilibrium particle flows with arbitrary number of phases. The fluid is added to the next example to simulate the effect both transport and drag. Different Stokes numbers are tested to comply with different physical properties of the fluid. For all the Stokes numbers, the initial particle density is given by

$$\rho(0,x) = e^{-25x^2},$$

and the initial particle velocity is

$$u(0,x) = -\sin(x)|\sin(x)|.$$

We test our method in the following simplified model

$$\partial_t f(t,x,\xi) + \xi\cdot\nabla_x f + \nabla_\xi\cdot(Ff) = 0, \tag{4.1}$$

$$\rho_f(\partial_t u + uu_x) = -\int m_p F(u,\xi) f d\xi, \tag{4.2}$$

where ρ_f denotes the fluid density and m_p is the droplet mass. Both ρ_f and m_p are assumed to be 1 for simplicity. The fluid velocity is set to be a constant, $u_f(x) = 1$. The initial fluid velocity is set to be a shock moving to right, i.e.,

$$u(0,x) = H(-x),$$

where $H(x)$ is the heaviside function. The linear drag force is hence

$$F(t,x) = (u(t,x)-\xi)/S_t, \quad S_t = 0.1, 1, 10, \cdots.$$

The fluid dynamic equation (4.2) is solved with a second order Runge-Kutta temporally and a finite volume scheme with a second order ENO flux limiter spatially. Here we simply take $\phi(0,x,\xi) = \xi - u(0,x)$ since particles are everywhere. A constant extension boundary condition for fluid velocity and particle density is used, while a periodic boundary condition is employed for the particle velocity.

Case 1: Stokes number $S_t = 0.1$.
When $S_t = 0.1$, the drag force is strong, so the particle will follow the fluid closely and no particle will cross at beginning. However, after 0.5 second, there will be PTC happening. Note that the particle density becomes very oscillatory due to the interaction between the particles and the fluid. Due the large drag force F, the fluid will not maintain a shock. At time $t = 0.5$, some oscillation also exhibits in the fluid. See in Fig. 3 for details.

Case 2: Stokes number $S_t = 1$
When S_t changes to 1, the drag force becomes weaker and we observe particles crossing each other as in Fig. 4. We observe that the particle becomes smoother and the fluid is less affected by the particles. However, near the shock the interaction between fluid and particle is still distinctly visible.

Case 3: Stokes number $S_t = 10$
When $S_t = 10$, the drag force is small, so the particles respond to the fluid very slowly and behave like the ones in free motion as we see in Fig. 5. Since the particle is less affected by the fluid, the particle trajectories cross in the simulation. We observe five particle velocities at time $t = 0.5$. This is also confirmed by the fluid velocity, which is close to the movement of shock. Due to the complex structure of the particle velocity, more nodes are needed if quadrature-based moment method is used. This example shows that initial uni-mode velocity will become multi-valued when PTC happens due the interaction between the fluid and the particles. The level set method captures all emerging velocity modes.

4.2. **Two-dimensional test cases.** *1. Crossing particle jets*
In this example, we demonstrate the ability of the level set method to capture particle crossing trajectories in two dimensional flows with infinite Stokes number particles.

Restricted in a unit box $\{x| \quad |x_1| \leq 0.5, |x_2| \leq 0.5\}$, two jets are initially concentrated in two separate regions

$$J_1 = \{x|\ 0.25 \leq x_1 \leq 0.5,\ |x_2| \leq 0.025\}, \quad J_2 = \{x||x_1| \leq 0.05,\ -0.5 \leq x_2 \leq -0.35\}.$$

The initial setting for these two jets can be described as

$$\rho_0(x) = 20\chi(J_1) + 20\chi(J_2), \quad u_0(x) = [-1, 0]\chi_{J_1} + [0, 1]\chi_{J_2}.$$

Initial data for the distribution is $f_0(x, \xi) = \rho_0(x, \xi)\delta(\phi_0(x, \xi))$. A distance function in (2.5) is used to initialize $\phi(0, x, \xi)$. $\rho(0, x, \xi)$ is initialized as $\rho_0(x)|\nabla_\xi \phi(0, x, \xi)|$. An impinging boundary condition is used to represent incoming particles in x direction.

We know that that when $t = 0.25$ two jets start to collide. We can clearly see the collision at time $t = 0.3$. When $t = 0.5$ two jets have crossed each other. Fig. 6 illustrates the time evolution of particle number density for crossing jets. Here the solid lines represent the exact solutions while the red dashed lines represents the numerical solutions. We see that the level set method indeed captures all the movement and crossing of particles.

Fig. 7 shows the density at time 0.5. Besides some numerical viscosity at the tips of the particle flows, it validates the quantitative correctness in recovering the particle density.

2. Particle wall rebound
In this example, we consider a particle flow bouncing off a reflective wall. Still restricted in a unit box $\{x| \quad |x_1| \leq 0.5, |x_2| \leq 0.5\}$, a particle jet is initially concentrated in the region

$$J = \{x|\ -0.5 \leq x_1 \leq -0.1,\ -0.55 \leq x_1 + x_2 \leq -0.45\}.$$

The initial setting for density is given by

$$\rho_0(x) = \chi_J$$

and for velocity by

$$u = [1 \quad -1] * \chi_J.$$

The particle with velocity $[1 \quad -1]$ will be bounced off at the wall $W_r = \{x| \quad x_2 = -0.5\}$ with velocity $[1 \quad e]$, $\quad 0 \leq e \leq 1$. Most moment closures use the average velocity $[1 \quad (e-1)/2]$ for convective transport, they are not able to reflect particles from the wall. For particles we use the reflective boundary condition

$$f(t,x,\xi_{\text{in}}) = f(t,x,\xi_{\text{out}}),$$

where

$$\xi_{out} = \xi_{\text{in}} - \alpha(\xi_{\text{in}} \cdot \nu(x))\nu(x)$$

with $\nu(x)$ the outer normal vector at the point $x \in \partial\Omega$ and α a reflective parameter. In this example $\nu(x) = (0,-1)^\top$ and $\alpha = 1+e$. Such a reflective boundary condition can be built in the level set method as [8].

Since the reflective wall is at $W_r = \{x| \quad x_2 = -0.5\}$, we can use the boundary condition

$$\phi(t,x,\xi_{in}) = \phi(t,x,\xi_{out}), \quad \rho(t,x,\xi_{in}) = \rho(t,x,\xi_{out}), \quad x \in W_r,$$

where

$$\xi_{in} = (\xi_1,\xi_2), \quad \xi_{out} = (\xi_1,-e\xi_2).$$

First we discretize the computational box with spatial step size Δx_1, Δx_2, $\Delta\xi_1$ and $\Delta\xi_2$. Numerically, a periodic extension according to the reflective boundary condition is used for determining the derivative with respect to x_2 at or near the rebounding wall W, e.g.,

$$D^-_{x_2}\phi(x_1,-0.5,\xi_1,\xi_2) = \frac{\phi(x_1,-0.5,\xi_1,-e\xi_2) - \phi(x_1,0.5-dx_2,\xi_1,-e\xi_2)}{\Delta x_2}.$$

At the incoming wall $W_i = \{x|x_1 = -0.05\}$, the particles are coming at the angle of $3\pi/4$. An angled incoming boundary condition for determining the derivative with respect to x_1 is enforced here. The idea is that, for each point outside of the computation domain, we need to find a point in the domain, which is constat along the particle flow. In case of particles coming at the angle of $3\pi/4$, we can compute the $D^-_{x_1}\phi$ at the boundary as

$$D^-_{x_1}\phi(-0.5,x_2,\xi_1,\xi_2) = \frac{\phi(-0.5,x_2,\xi_1,\xi_2) - \phi(-0.5,x_2-dx_2,\xi_1,\xi_2)}{\Delta x_1}.$$

The density contours are plotted in Fig. 8. It clearly shows the movement and rebouncement of the particle flow. This example demonstrates that the physical conditions, such as incoming, crossing, rebouncing, etc., can be built into the level set formulation and implementation.

5. Concluding Remarks

A level set approach for kinetic equations of sprays has been derived and verified for non-equilibrium, dilute, fluid particle flows. The method can successfully handle flows with particle-crossing trajectories and thus is able to compute accurately particle velocity statistics in an Eulerian framework. In addition to applications involving dispersed-phase flows, the proposed method should find use in some other applications governed by kinetic equations.

Acknowledgments

This research was supported by the National Science Foundation under Grant DMS05-05975.

References

[1] A. Amsden, J. Ramshaw, P. ORourke, and J. Dukowicz. A computer program for two- and three-dimensional fluids flow with chemical sections and fuel sprays. *Los Alamos*, 1985.

[2] C. Baranger. Modelling of oscillations, breakup and collisions for droplets: the establishment of kernels for the T.A.B. model. *Math. Models Methods Appl. Sci.*, 14(5):775–794, 2004.

[3] C. Baranger, L. Boudin, P.-E. Jabin, and S. Mancini. A modeling of biospray for the upper airways. In *CEMRACS 2004—mathematics and applications to biology and medicine*, volume 14 of *ESAIM Proc.*, pages 41–47 (electronic). EDP Sci., Les Ulis, 2005.

[4] C. Baranger and L. Desvillettes. Coupling Euler and Vlasov equations in the context of sprays: the local-in-time, classical solutions. *J. Hyperbolic Differ. Equ.*, 3(1):1–26, 2006.

[5] L. Boudin and L. Weynans. Spray impingement on a wall in the context of the upper airways. In *CEMRACS 2004—mathematics and applications to biology and medicine*, volume 23 of *ESAIM Proc.*, pages 1–9. EDP Sci., Les Ulis, 2008.

[6] J. Carrilo and T. Goudon. Stability and asymptotic analysis of a fluid-particles interaction model. *Comm. PDE*, 31:1349–1379, 2006.

[7] J. Carrilo, T. Goudon, and P. Lafitte. Simulation of fluid and particles flows: Asymptotic preserving schemes for bubbling abd flowing regimes. *J. COmp. Phys.*, 227:7929–7951, 2008.

[8] L.-T. Cheng, M. Kang, S. Osher, H. Shim, and Y.-H. Tsai. Reflection in a level set framework for geometric optics. *CMES Comput. Model. Eng. Sci.*, 5(4):347–360, 2004.

[9] K. Desjardins and P. Villedieu. A hierarchy of models for turbulent dispersive two-phase flows derived from a kinetic equation for the joint particle-gas. *Comm. Math. Sci.*, 5:331–353, 2007.

[10] O. Desjardins, R. O. Fox, and P. Villedieu. A quadrature-based moment method for dilute fluid-particle flows. *J. Comput. Phys.*, 227(4):2514–2539, 2008.

[11] R. B. Diemer and J. H. Olson. A moment methodology for coagulation and breakage problems: Part 2 - moment models and distribution reconstruction,. *Chem. Eng. Sci.*, 57:2211, 2002.

[12] K. Domelevo and J.-M. Roquejoffre. Existence and stability of travelling wave solutions in a kinetic model of two-phase flows. *Comm. Partial Differential Equations*, 24(1-2):61–108, 1999.

[13] J. K. Dukowicz. A particle-fluid numerical model for liquid sprays. *J. Comput. Phys.*, 35(2):229–253, 1980.

[14] T. Elperin, N. Kleeorin, I. Rogachevskii, and D. Sokoloff. Turbulent transport of atmospheric aerosols and formation of large-scale structure. *Phys Chem Earth*, A25:797–803, 2000.

[15] R. Fan, D. L. Marchisio, and R. O. Fox. Application of the direct quadrature method of moments to polydisperse gas-solid fluidized beds. *Powder Technology*, 139:7, 2004.

[16] R. O. Fox. *Computational models for turbulent reacting flows*. Cambridge University Press, Cambridge, 2003.

[17] R. O. Fox. Bivariate direct quadrature method of moments for coagulation and sintering of particle populations. *Journal of Aerosol Science*, 37:1562, 2006.

[18] R. O. Fox, F. Laurent, and M. Massot. Numerical simulation of spray coalescence in an Eulerian framework: direct quadrature method of moments and multi-fluid method. *J. Comput. Phys.*, 227(6):3058–3088, 2008.

[19] M. Golomboka and D. B. Pyea. Droplet dynamics in a diesel injection spray. *Fuel*, 69(9):1200–1202, 1990.

[20] T. Goudon and F. Poupaud. On the modeling of the transport of particles in turbulent flows. *M2AN Math. Model Numer. Anal.*, 38:673–690, 2004.

[21] K. Hamdache. Global existence and large time behaviour of solutions for the Vlasov-Stokes equations. *Japan J. Indust. Appl. Math.*, 15(1):51–74, 1998.

[22] H. M. Hulburt and S. Katz. Some problems in particle technology. *Chem. Eng. Sci.*, 19:555, 1964.

[23] S. Jin, H. Liu, S. Osher, and R. Tsai. Computing multi-valued physical observables for the high frequency limit of symmetric hyperbolic systems. *J. Comput. Phys.*, 210(2):497–518, 2005.

[24] S. Jin, H. Liu, S. Osher, and Y.-H. R. Tsai. Computing multivalued physical observables for the semiclassical limit of the Schrödinger equation. *J. Comput. Phys.*, 205(1):222–241, 2005.

[25] F. Laurent and M. Massot. Multi-fluid modeling of laminar polydisperse spray flames: origin, assumptions and comparison of sectional and sampling methods. *Combust. Theory Modelling*, 15(5):537–542, 2001.

[26] H. Liu, S. Osher, and Y.-H. R. Tsai. Multi-valued solution and level set methods in computational high frequency wave propagation. *Comm. Compu. Phys.*, 1(5):765–804, 2006.

[27] H. Liu and Z. Wang. Superposition of multi-valued solutions in high frequency wave dynamics. *J. Sci. Comput.*, 35(2-3):192–218, 2008.

[28] D. L. Marchisio and R. O. Fox. Solution of population balance equations using the direct quadrature method of moments. *Journal of Aerosol Science*, 36:43–73, 2005.

[29] R. McGraw. Description of aerosol dynamics by the quadrature method of moments. *Aerosol Science and Technology*, 27:255, 1997.

[30] S. Osher and J. A. Sethian. Fronts propagating with curvature-dependent speed: algorithms based on Hamilton-Jacobi formulations. *J. Comput. Phys.*, 79(1):12–49, 1988.

[31] L. Sainsaulieu. Equilibrium velocity distribution functions for a kinetic model of two-phase flows. *Math. Models Methods Appl. Sci.*, 5(2):191–211, 1995.

[32] L. Schiller and A. Nauman. A drag coefficient correclation. *V. D. I. Zeitung*, 77:318–320, 1935.

[33] F. A. Williams. *Combustion theory*. Benjamin Cummings Publ., 1985.

FIGURE 1. Multiple velocity and averaged density at time about 0.1, 0.2, 0.3 and 0.4.

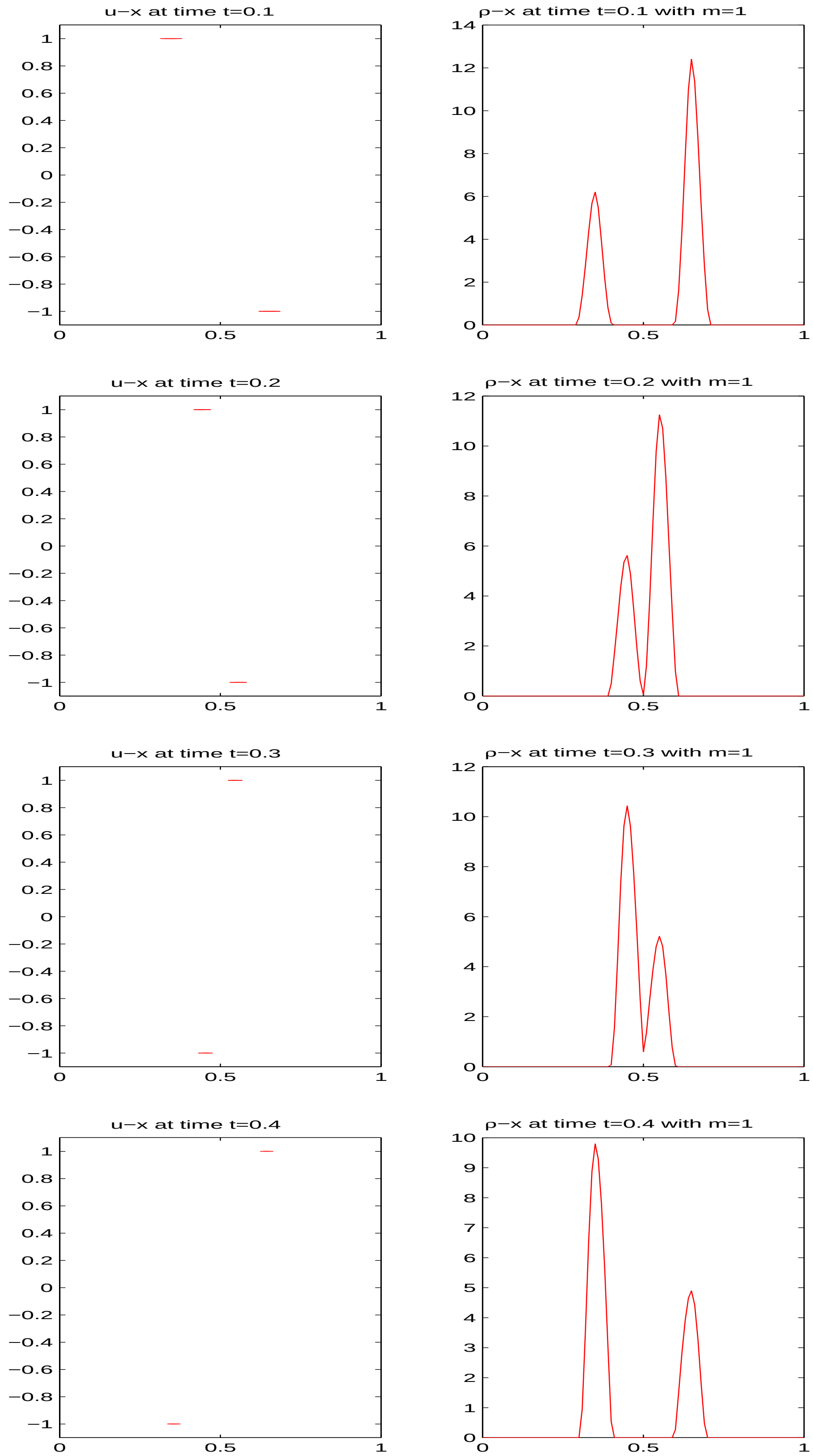

FIGURE 2. Multiple velocity and total density at time about 0.1, 0.5, 0.7 and 1.0.

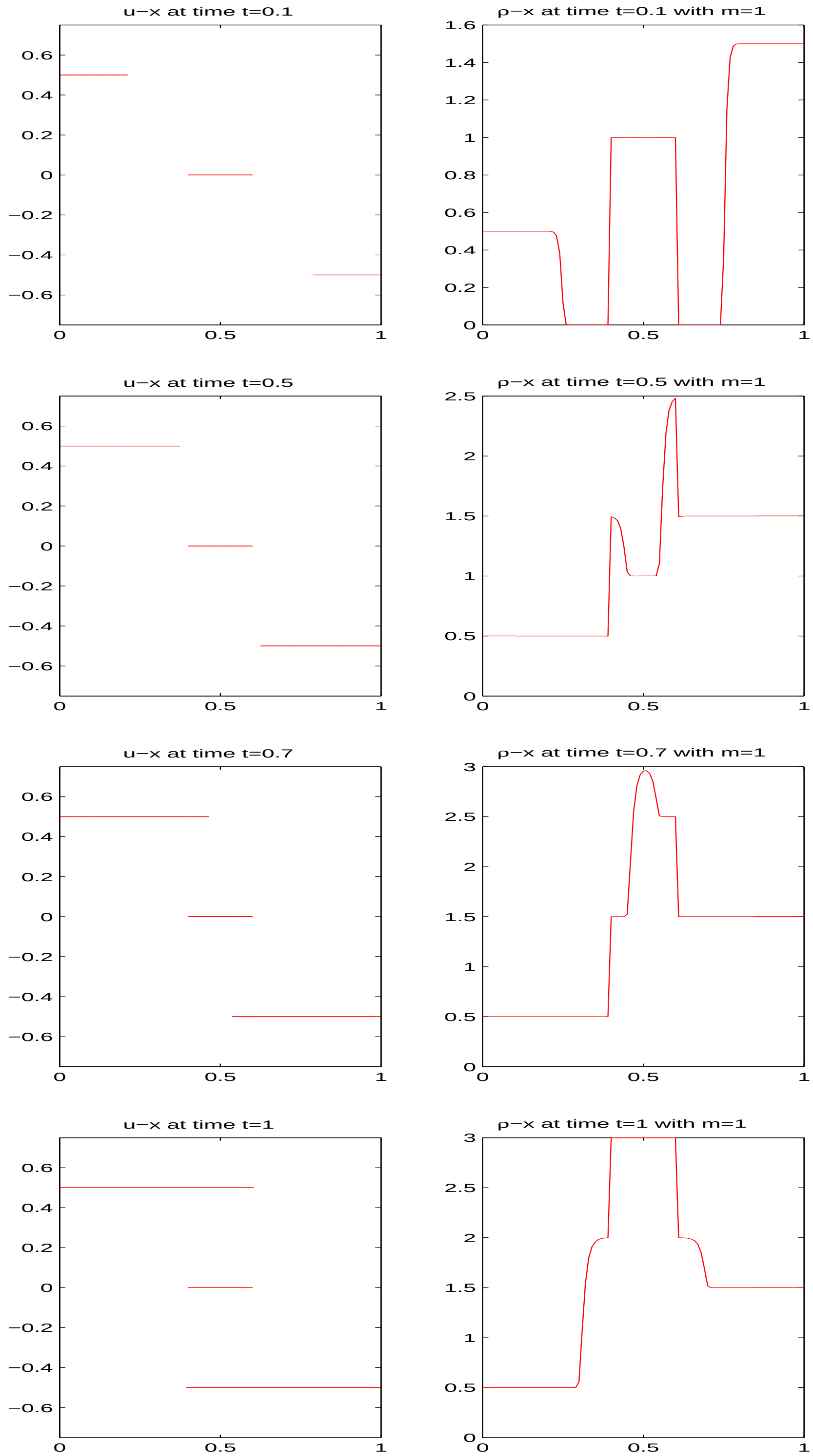

FIGURE 3. velocity, particle velocity and particle density at time $t = 0.1$, 0.2 and 0.5 for $S_t = 0.1$

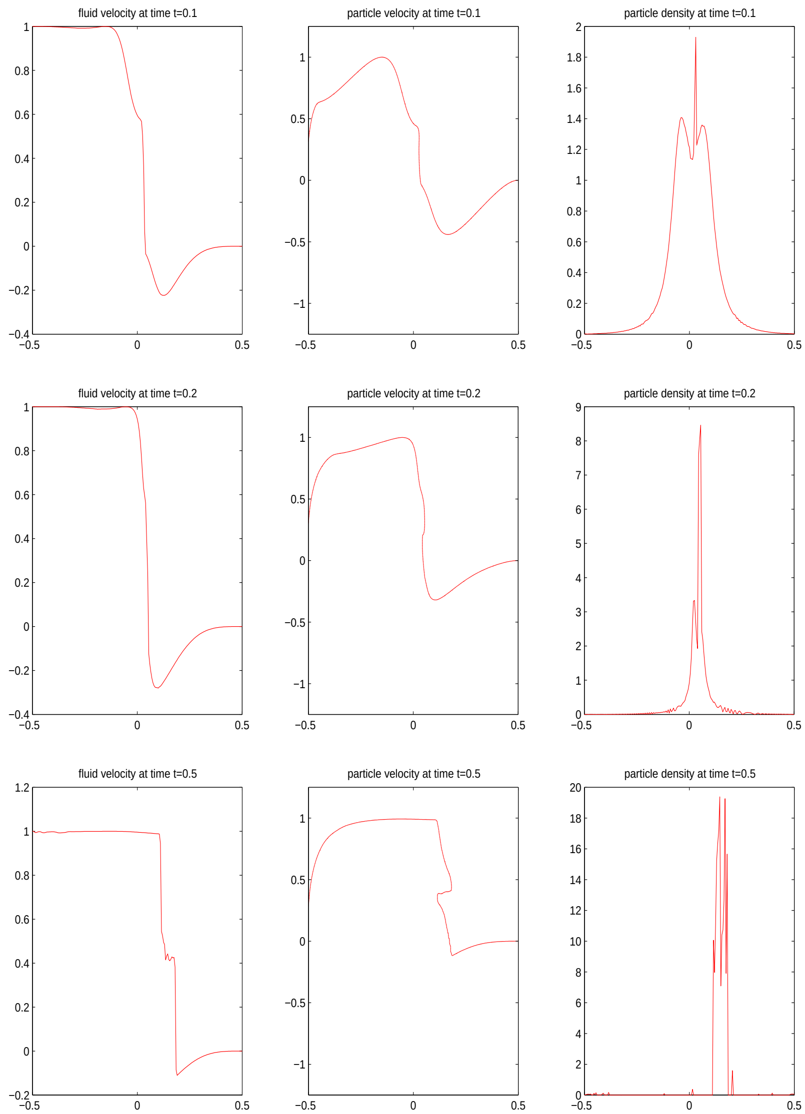

FIGURE 4. velocity, particle velocity and particle density at time $t = 0.1$, 0.2 and 0.5 for $S_t = 1$

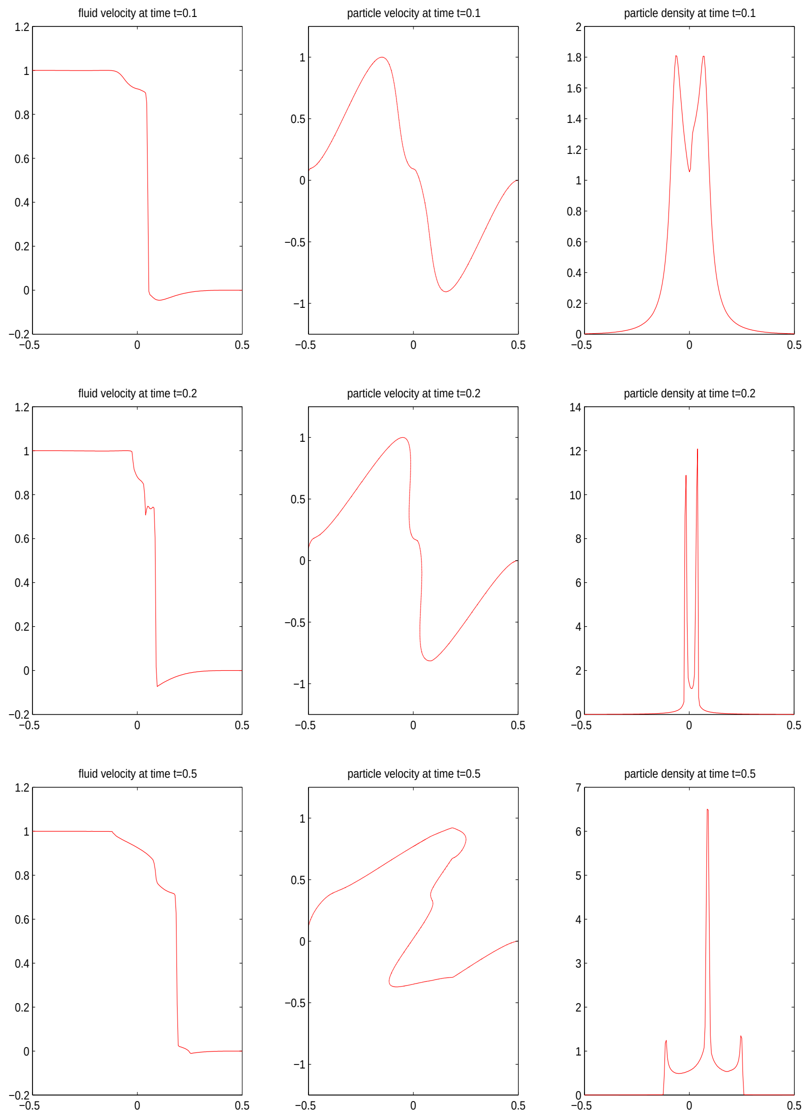

FIGURE 5. Fluid velocity, particle velocity and particle density at time $t = 0.1$, 0.2 and 0.5 for $S_t = 10$

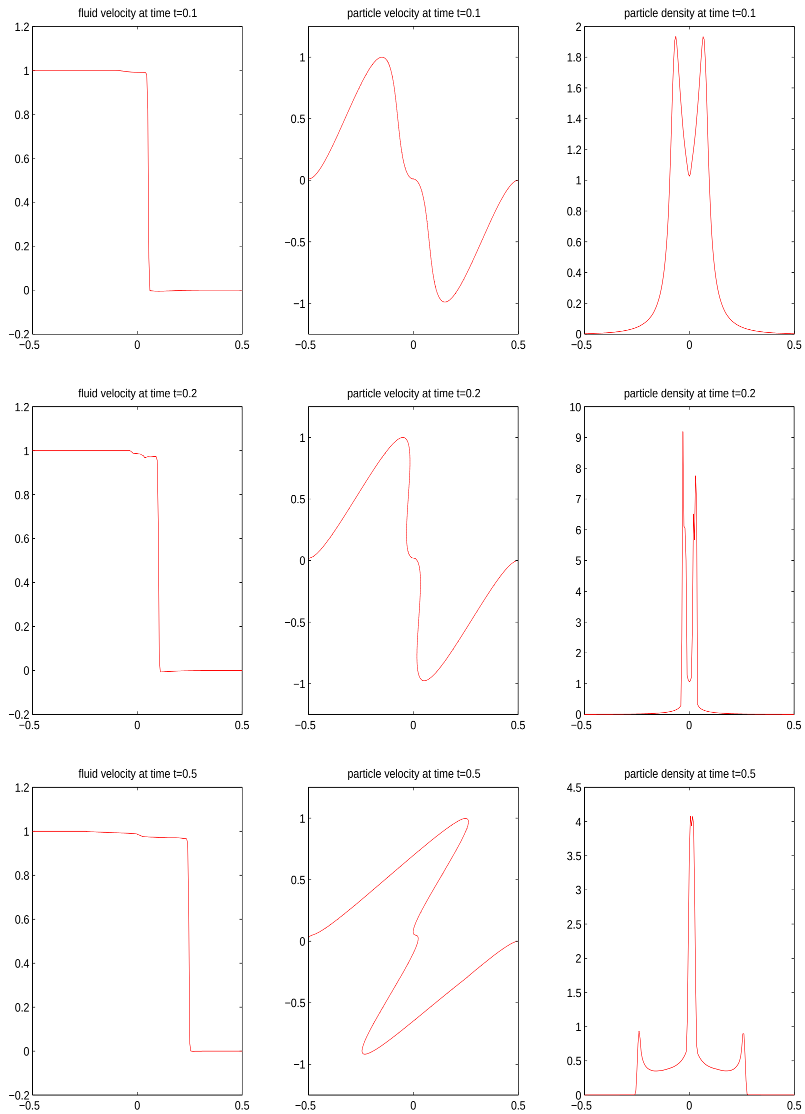

FIGURE 6. Density contour at time about 0.1, 0.3 and 0.5.

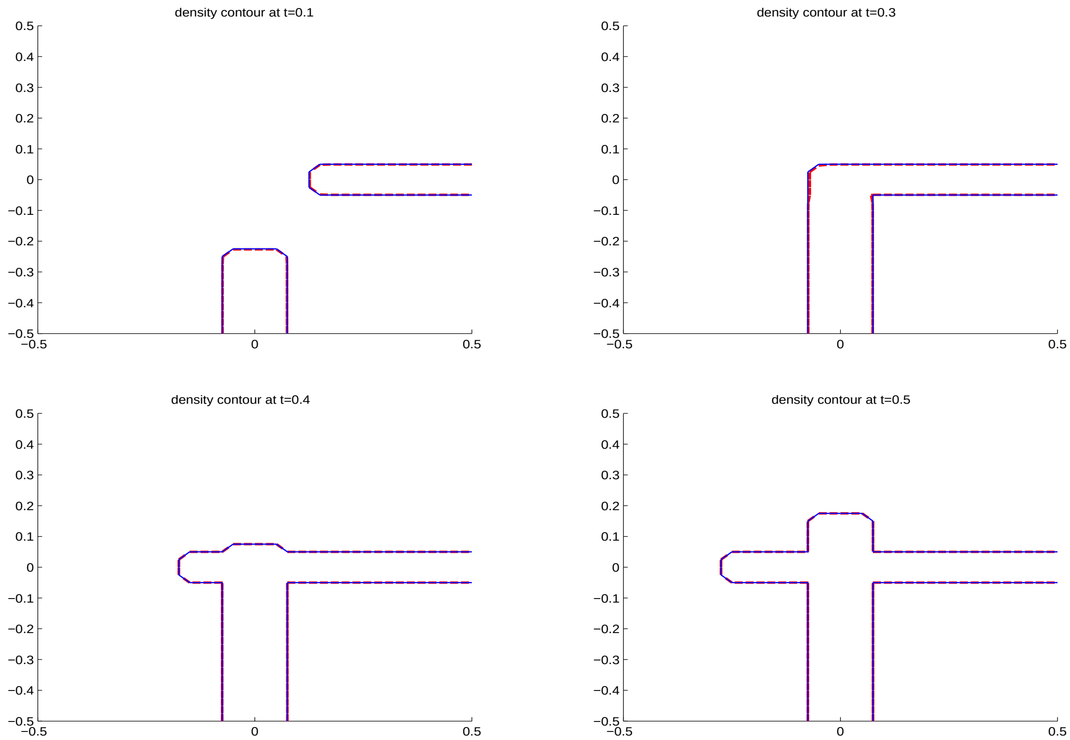

FIGURE 7. Density at time 0.5.

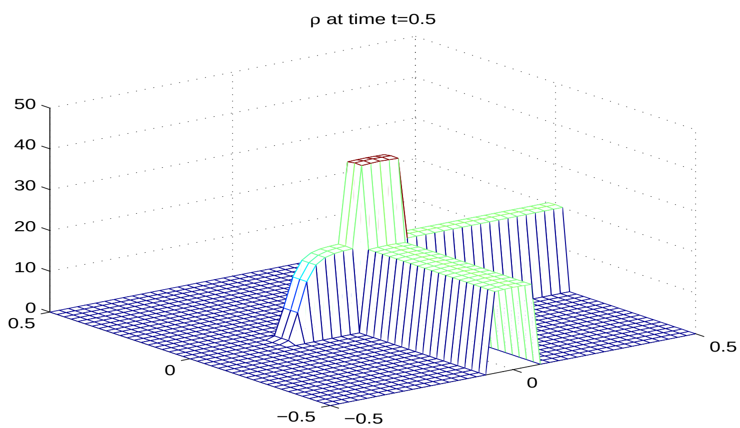

FIGURE 8. Density contour at time about 0.1, 0.2, 0.3 and 0.4.